

## Original Article

# Xp11.2 translocation/TFE3 gene fusion renal cell carcinoma with a micropapillary pattern: cases report and literature review

Zhou-Yi Xu<sup>1\*</sup>, Jing-Ping Wang<sup>1\*</sup>, Yu Zhang<sup>1\*</sup>, Shi-Wu Wu<sup>1</sup>, Li Ma<sup>1</sup>, Yan-Zi Qin<sup>1</sup>, Z Peter Wang<sup>2,3</sup>, Da-Min Chai<sup>1</sup>, Yi-Sheng Tao<sup>1</sup>

<sup>1</sup>Department of Pathology, The First Affiliated Hospital of Bengbu Medical College, Bengbu Medical College, Bengbu, Anhui, China; <sup>2</sup>Department of Biochemistry and Molecular Biology, School of Laboratory Medicine, Bengbu Medical College, Anhui, Bengbu 233030, China; <sup>3</sup>Department of Pathology, Beth Israel Deaconess Medical Center, Harvard Medical School, Boston, MA, USA. \*Equal contributors.

Received July 25, 2018; Accepted December 18, 2018; Epub January 15, 2019; Published January 30, 2019

**Abstract:** Xp11.2 translocation/transcription factor E3 (TFE3) gene fusion renal cell carcinoma (Xp11.2 translocation RCC) was first classified as a distinct type of renal tumor by the World Health Organization in 2004. However, its morphology and clinical manifestations often overlap with those of conventional RCCs. Moreover, a micropapillary pattern (MPP) comprising small papillary cell clusters surrounded by lacunar spaces has never been described in RCC. We compared the clinicopathological and prognostic characteristics of one patient with Xp11.2 translocation RCC exhibiting an MPP (TFE3-M) to those of four patients with conventional Xp11.2 translocation RCC (TFE3-N); all five tumors resembled conventional RCCs on gross pathology. All patients exhibited similar histologies, clinical manifestations, and prognoses, and all underwent radical nephrectomy. However, their characteristics differed significantly from those of other MPP-comprising neoplasms. Both tumor types were positive for TFE3 and vimentin; however, TFE3-M tumor cells expressed epithelial membrane antigen and human melanoma black-45 but not cluster of differentiation 10 (CD10), whereas the TFE3-N cells expressed P504S, CD10, and vimentin but not cytokeratin 7. Our RT-PCR analysis result showed that TFE3-N and TFE3-M tumor cells were identified expressing *ASPSCR1-TFE3* and *PRCC-TFE3* fusion genes, respectively. These findings suggest that TFE3-M should be classified as a histological subtype of Xp11.2 translocation RCC, although its relationship with other MPP-exhibiting neoplasms remains unclear. The histological characteristics of Xp11.2 translocation RCCs depend on MiT family transcription factors and their gene fusion partners. Xp11.2 translocation RCC should be considered for malignancies presenting with a particular pattern; such malignancies can be identified reliably by their morphological and immunohistochemical profiles.

**Keywords:** TFE3, renal cell carcinoma, micropapillary pattern, morphology, diagnosis

## Introduction

Xp11.2 translocation/transcription factor E3 (TFE3) gene fusion renal cell carcinoma (Xp11.2 translocation RCC) was first described as a new entity in the World Health Organization (WHO) renal tumor classification of 2004. This disease is characterized by a gene fusion resulting from the translocation of *TFE3* on chromosome Xp11.2 to another chromosome. Notably, the morphology and clinical manifestations of Xp11.2 translocation RCC often overlap with those of conventional renal carcinoma [1, 2].

Pathologically, a micropapillary pattern (MPP) comprises small papillary cell clusters surrounded by lacunar spaces. In 1997, Silver and Askin first reported the presence of an MPP in pulmonary adenocarcinoma and described it as a strongly invasive malignancy [3]. Another study showed that lymph node and distant metastases were common features of this type of tumor, and that this disease had a higher risk of postoperative recurrence than conventional pulmonary adenocarcinoma [4]. Although MPPs have since been described in other cancers including breast, ovarian, and colon cancer [5],

**Table 1.** Clinicopathological characteristics of the cases

Case	Type	Sex	Age (years)	Location	Size (cm)*	Follow-up (months)	Follow-up result	Initial symptoms	Immunotherapy (months)
1	TFE3-N	F	19	Right kidney	10	38	NR	Right-sided back pain for 2 weeks	3
2	TFE3-N	M	23	Left kidney	5	40	NR	Physical examination found an occupying lesion in the left kidney	3
3	TFE3-N	F	59	Left kidney	5	5	NR	Painless hematuria for 2 months	1
4	TFE3-N	M	48	Right kidney	4	7	NR	Right-sided back pain for 3 months	3
5	TFE3-M	M	30	Left kidney	6	4	NR	Hematuria for 4 days	3

\*Largest diameter of the tumor. F, female; M, male; NR, no recurrence; TFE-N, Xp11.2 translocation renal cell carcinoma (RCC) with a normal pattern; TFE-M, Xp11.2 translocation RCC with a micropapillary pattern.

there have been no reports of this pattern in RCCs to date.

In this case series, we analyzed five patients with Xp11.2 translocation RCC, including one with an MPP (TFE3-M). We compared the clinicopathological, immunohistochemical, imaging, clinical, and prognostic characteristics of the patient with TFE3-M RCC to those with the conventional pattern Xp11.2 translocation (TFE3-N) RCC to improve our understanding of these RCC types and increase awareness of RCCs exhibiting an MPP.

## Materials and methods

### Patients and tissue samples

Five patients with Xp11.2 translocation RCC treated at the Department of Pathology of the First Affiliated Hospital of the Bengbu Medical College between November 2014 and October 2017 were included in this series. The selected patients had not received radiotherapy, chemotherapy, or immunotherapy before undergoing radical nephrectomy. Complete clinical and pathological data were obtained from all five patients, and tissue samples were obtained during surgery. The study was approved by the ethics committee of Bengbu Medical College, and all patients provided written informed consent.

### Immunohistochemistry

All tissue specimens were fixed in 10% buffered formalin and embedded in paraffin. Continuous 4  $\mu$ m-thick tissue sections were cut, deparaffinized, dehydrated with xylene, and graded with ethanol. Primary antibodies specific for transcription factor E3 (TFE3), P504S, epithelial membrane antigen (EMA), cluster of differentiation 10 (CD10), vimentin, cytokeratin 7 (CK7), renal cell carcinoma (RCC), and human mela-

noma black 45 (HMB45), as well as a 3'-diaminobenzidine (DAB) staining kit, were purchased from Fuzhou Maixin Biotechnology Co., Ltd. (Fuzhou, China). Immunohistochemistry was performed using the Elivision™ Plus detection kit (LabVision, Fremont, CA, USA) according to the manufacturer's instructions. The sections were stained with DAB, re-stained with hematoxylin and eosin, dehydrated, air-dried, and mounted. Phosphate-buffered saline was used instead of the primary antibody as a negative control, and a known positive section supplied with the antibody by the manufacturer was used as a positive control.

### Evaluation of the staining results

EMA, CD10, and RCC were localized in the cytoplasm and cell membrane; P504s, vimentin, CK7, and HMB-45 were localized in the cytoplasm, while TFE3 was localized in the cytoplasm and nucleus. P504s and RCC are nephrogenic tumor markers, while EMA is an epithelial marker, CD10 a germinal center marker, and HMB-45 a melanoma marker. CK7 can be used to distinguish conventional RCC from chromophobe cell carcinoma.

The immunohistochemistry results were scored based on both the staining intensity (none: 0; weak: 1; moderate: 2; and strong: 3) and extent (< 11%: 1; 11-50%: 2; 51-75%: 3; and > 75%: 4) using previously a published scoring method [6]. The intensity and extent scores were then multiplied to yield final scores that ranged from 0 to 12; scores  $\geq 3$  were considered positive. The results were interpreted by two independent pathologists using the double-blind method. For each patient sample, 50 cells per visual field were selected 400 times for image acquisition. The cells were counted using the ImageJ software (National Institutes of Health, Bethesda, MD, USA) (Table 2). Cell counting was performed as follows: First, the acquired

**Table 2.** Cytological features

Case	Total number of cells*	Central nucleoli, n*	Central nucleoli, %	Side nucleoli, n*	Side nucleoli, %	Heteromorphic nuclei, n*	Heteromorphic nuclei, %	Multiple nucleoli, n*	Multiple nucleoli, %
1	15,388	982	6.38	1,593	10.35	116	0.75	674	4.38
2	17,725	149	0.84	635	3.58	37	0.21	182	1.03
3	7,854	516	6.57	1,090	13.89	348	4.44	218	2.78
4	11,293	262	2.32	1,034	9.16	54	0.48	271	2.4
5	3,133	235	7.5	459	14.65	200	6.38	91	2.9

\*A total of 50 cell visual fields were selected for each case (magnification:  $\times 400$ ), and the number of total cells was analyzed.

photograph was converted into a 'type 8-bit image'; next, the image brightness and contrast were enhanced to increase its overall contrast, following which the image was inverted using the 'Invert' function. The image's 'threshold' was then adjusted until the particles were adequately distinguishable from the background. Finally, a number of cells were obtained via the 'Summarize' command.

#### RT-PCR

Reverse transcription polymerase chain reaction (RT-PCR) was used to determine the karyotypes by detecting the expression of fusion gene. We first used an RNeasy FFPE kit (Qiagen, Valencia, CA, USA) to extract RNA from formalin fixed-paraffin embedded tissue sections. Next, the RNA was reverse transcribed to generate cDNA using an M-MLV reverse transcriptase (Promega, Madison, WI, USA). Then, PCR was performed using an Ex Taq Polymerase (Takara Bio, Otsu, Japan). Finally, the PCR products were electrophoresed in an agarose gel (Sigma-Aldrich, St Louis, MO, USA). The gel was visualized in an ultraviolet transilluminator and recorded by photography. All steps were performed according to the manufacturer's instructions. Primers were designed to amplify two of the known translocation types (*ASPSCR1-TFE3* and *PRCC-TFE3*) [7]. The specific primer sequences were as follows: *ASPSCR1-TFE3* (FORW: AAA GAA GTC CAA GTC GGG CC, REV: CGT TTG ATG TTG GGC AGC TC); *PRCC-TFE3* (FORW: GCC TCA ATC TGC CCC CTC CAA T, REV: CGA GTG TGG TGG ACA GGT ACT).

#### Results

##### *Clinicopathologic characteristics of patients with Xp11.2 translocation RCC*

The main clinicopathological features of the five patients are shown in **Table 1**; three were men and two were women with ages ranging

from 19 to 58 years (median, 30 years). The lesions were located in the left and right kidney in three and two cases, respectively. Back pain and hematuria were the main clinical symptoms.

All five patients were treated with radical nephrectomy. Patients 1 and 2 were diagnosed and underwent surgery in 2014, and each received three rounds of postoperative immunotherapy. These patients returned to the hospital for renal function examinations and color doppler ultrasonography of the kidney every six months. To date, all tests have yielded normal findings and both patients have remained in good health without recurrence. Patients 3, 4, and 5 were diagnosed and underwent surgery in 2017. Patients 4 and 5 received immunotherapy for three months, while patient 3 stopped immunotherapy after 1 month because of lack of tolerance. Due to recently having undergone surgery, none of these three patients were subjected to renal function examination or color doppler ultrasonography of the kidney at the time of this study. To date, all three patients have remained in good health without recurrence.

##### *Imaging examinations*

With respect to the four patients with TFE3-N, computed tomography (CT) in patient 1 revealed inhomogeneous enhancement of the right kidney mass and a space-occupying lesion in the right renal capsule. Intravenous pyelography indicated normal excretion in both kidneys and circle-shaped opacities in the inferior pole of the right kidney. Angiography revealed multiple occupancies in the right kidney. In patient 2, CT indicated a potentially malignant space-occupying lesion in the left kidney. In patient 3, the structures of the renal pelvis and calices could not be distinguished clearly on urinary radiography, and partial erosions appeared to



**Figure 1.** Representative computed tomography images of Xp11.2 translocation renal cell carcinoma (RCC). A. A space-occupying lesion in the inferior pole of the right kidney (patient 4). B. A space-occupying lesion in the left kidney suggestive of a cystic RCC (patient 5). C. A mass resected from the pole of the kidney, with a greyish-brown cut surface accompanied by hemorrhage and necrosis (patient 5).

have affected renal performance. In patient 4, CT revealed a space-occupying lesion in the inferior pole of the right kidney (**Figure 1A**).

In patient 5 (with TFE3-M RCC), color doppler ultrasonography indicated a cystic mass in the left kidney. Subsequently, CT showed a space-occupying lesion in the left kidney that was determined to be a cystic RCC (**Figure 1B**). Emission CT indicated that the kidney was retaining normal excretory function.

#### Gross tumor characteristics

Although most tumors were single nodular masses, patient 1 presented with two separate nodules; one was located at the renal hilum and the other was contralateral to it. The lesions were located at a single pole of the kidney in patients 2, 4, and 5 and at the center of the kidney in patient 3. The lesions ranged in size from 4.0 to 10.0 cm (mean, 6 cm), and from greyish-white in color to greyish-brown. The cut surfaces of the tumors in patients 1 and 5 exhibited hemorrhaging and necrosis (**Figure 1C**).

#### Morphologic features

**Patient 1 (TFE3-N):** The neoplasm exhibited a papillary structure containing axons composed of fibers and blood vessels. The neoplastic cells had clear or eosinophilic cytoplasm. Cells with clear cytoplasm exhibited clear cell boundaries and unclear nucleoli, whereas those with eosinophilic cytoplasm had clear nucleolar atypia but unclear cell boundaries. In some areas, the

boundaries of cells with eosinophilic cytoplasm could be observed, and the karyoplasm ratio was unbalanced (**Figure 2A** and **2B**).

**Patient 2 (TFE3-N):** This patient's neoplasm exhibited a morphology typical of Xp11.2 translocation RCCs, with a papillary architecture and abundant clear-to-finely granular eosinophilic cytoplasm in the cells. The neoplasm-associated nucleoli were of a low grade and demonstrated a palisade structure (**Figure 2C**).

**Patient 3 (TFE3-N):** The neoplasm comprised crowded cells with a papillary structure. The cells exhibited a pseudostratified arrangement and contained high-grade neoplastic nucleoli. The cytoplasm in this patient's cells contained more eosinophilic granules than those in patient 2. Compared to patients 1 and 2, the neoplastic activity in this patient's tumor was associated with the intensity and extent of eosinophilic granules in the cytoplasm (**Figure 2D**).

**Patient 4 (TFE3-N):** this tumor exhibited a combination of nested and papillary architecture as well as a predominantly granular eosinophilic cytoplasm. In some areas, the neoplasm's morphology was significantly heteromorphic with a pseudo-adenoid structure (**Figure 2E**).

**Patient 5 (TFE3-M):** This neoplasm had an MPP component characterized by small papilla interspersed with acini and lacunae. Significant melanin particle deposition was observed in these spaces. The cells of the MPP component contained small-to-moderate amounts of eosino-

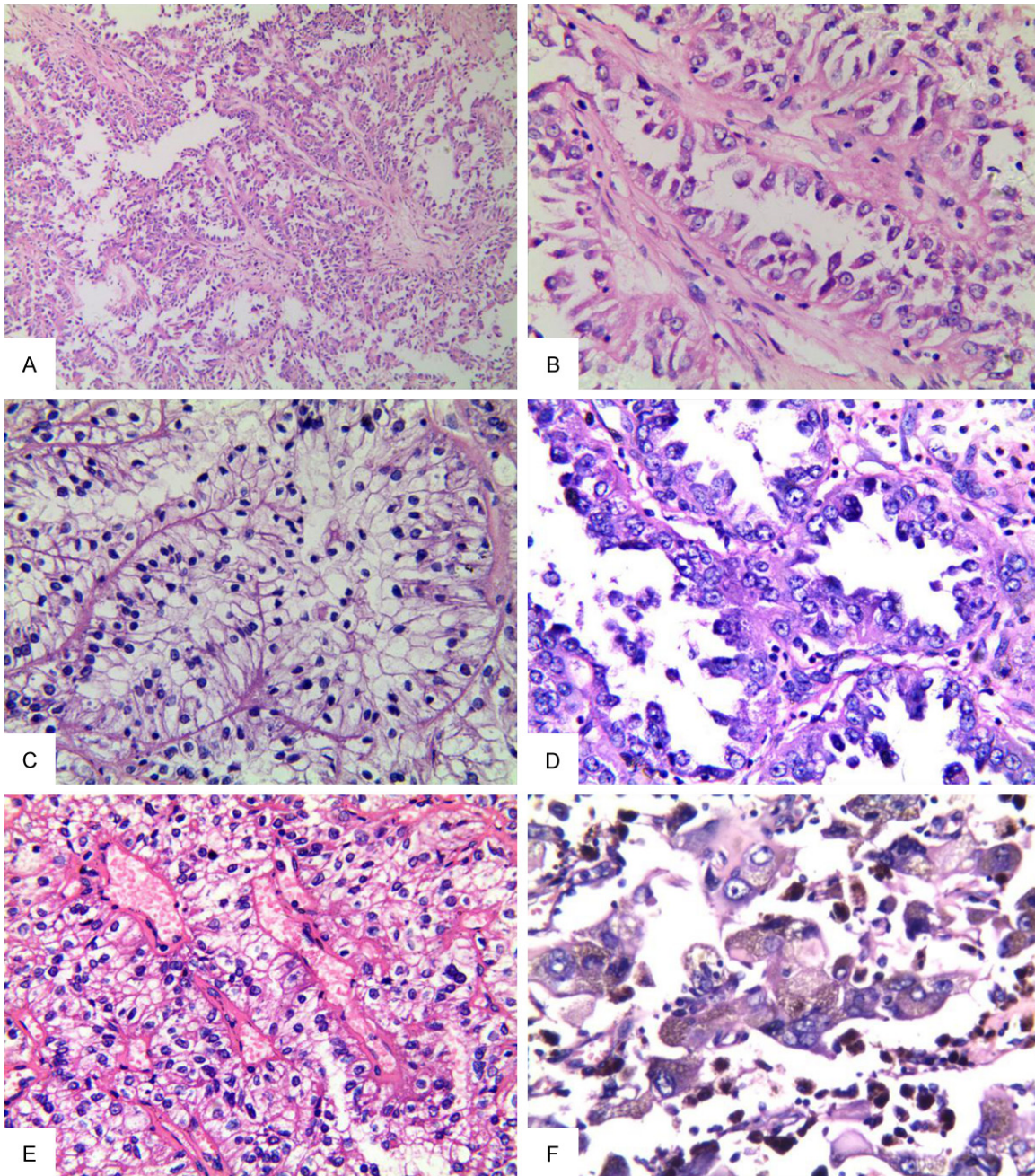


**Figure 2.** Morphological features of Xp11.2 translocation renal cell carcinoma (RCC). All images are of hematoxylin and eosin-stained tissues. (A) A neoplasm with a papillary structure at low magnifications (patient 1). (B) The neoplasm exhibited a papillary structure containing axons composed of fibers and blood vessels. Cells with eosinophilic cytoplasm had clear nucleolar atypia but unclear cell boundaries at high magnification (patient 1). (C) A neoplasm exhibiting the typical morphology of Xp11 translocation RCC (patient 2), including a papillary architecture and abundant clear-to-finely granular eosinophilic cytoplasm. (D) A neoplasm with crowded cells and a papillary structure (patient 3). The neoplastic nucleolar grade was high. (E) A tumor comprising a combination of nested and papillary architecture as well as a predominantly granular eosinophilic cytoplasm (patient 4). (F) Hematoxylin and eosin (HE) staining: The neoplasm exhibited a micropapillary pattern characterized by small papillae interspersed within the acini and lacunae. Significant melanin particle deposition was observed in the spaces in TFE3-M case (patient 5). Magnification:  $\times 100$  (A);  $\times 400$  (B-F).

philic cytoplasm. The tumor cells featured obvious nucleoli and had the highest percentage of

heterotypic cells among any of the five patients' samples (**Figure 2F; Table 2**).

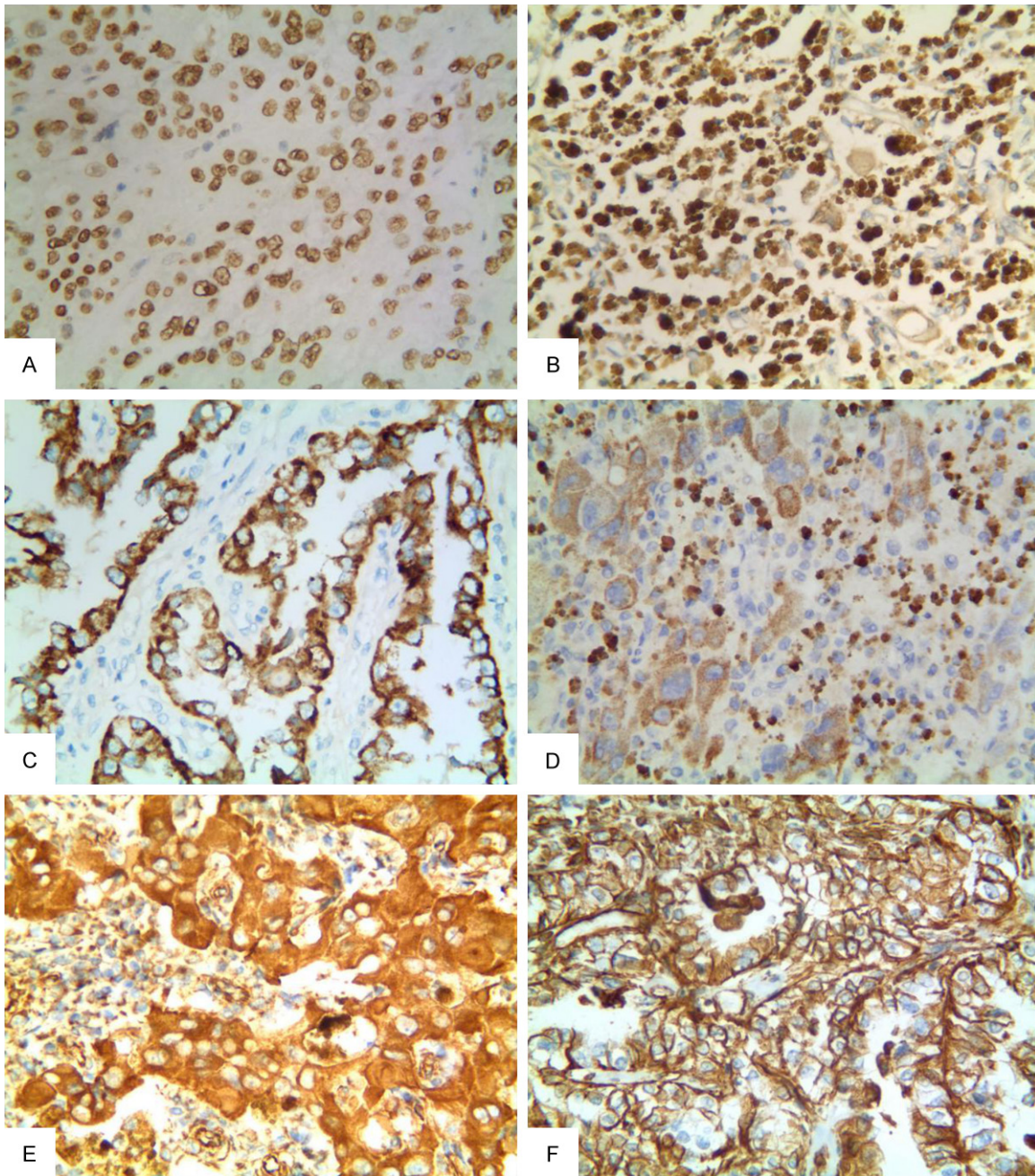


**Figure 3.** The immunohistochemical features of TFE3, P504S and vimentin in Xp11.2 translocation renal cell carcinoma (RCC). A. The nucleus showed strong, diffuse staining (dark brown) for transcription factor E3 (TFE3), with obvious nuclear membrane and nucleoli localization in TFE3-N case (patient 1). B. Transcription factor E3 (TFE3) was strongly expressed in the nucleus (dark brown) in TFE3-M case (patient 5). C. The cell membrane and cytoplasm were strongly positive for P504S, with staining of the cell membrane more intense than that of the cytoplasm in TFE3-N case (patient 3). D. P504S is positively expressed in the cytoplasm (light brown) in TFE3-M case (patient 5). E. The expression of vimentin was extensive and strong in the nucleus and cytoplasm (dark brown) and was more intense than in the TFE3-N group. Meanwhile, cell membrane staining was not obvious in TFE3-M case (patient 5). F. A strong positive expression of vimentin (dark brown) was observed in the cell membranes. The axial fibers in the papillary structure were also stained in TFE3-N case (patient 4). All magnifications:  $\times 400$ .

#### Immunohistochemistry

The tumor cells from all patients strongly expressed TFE3 and P504S (Figure 3A-D); some

expressed vimentin (Figure 3E and 3F), RCC (Figure 4A-C) and EMA (Figure 4D-F). Only the patient with TFE3-M exhibited weakly positive CK7 expression (Figure 5A), whereas patients

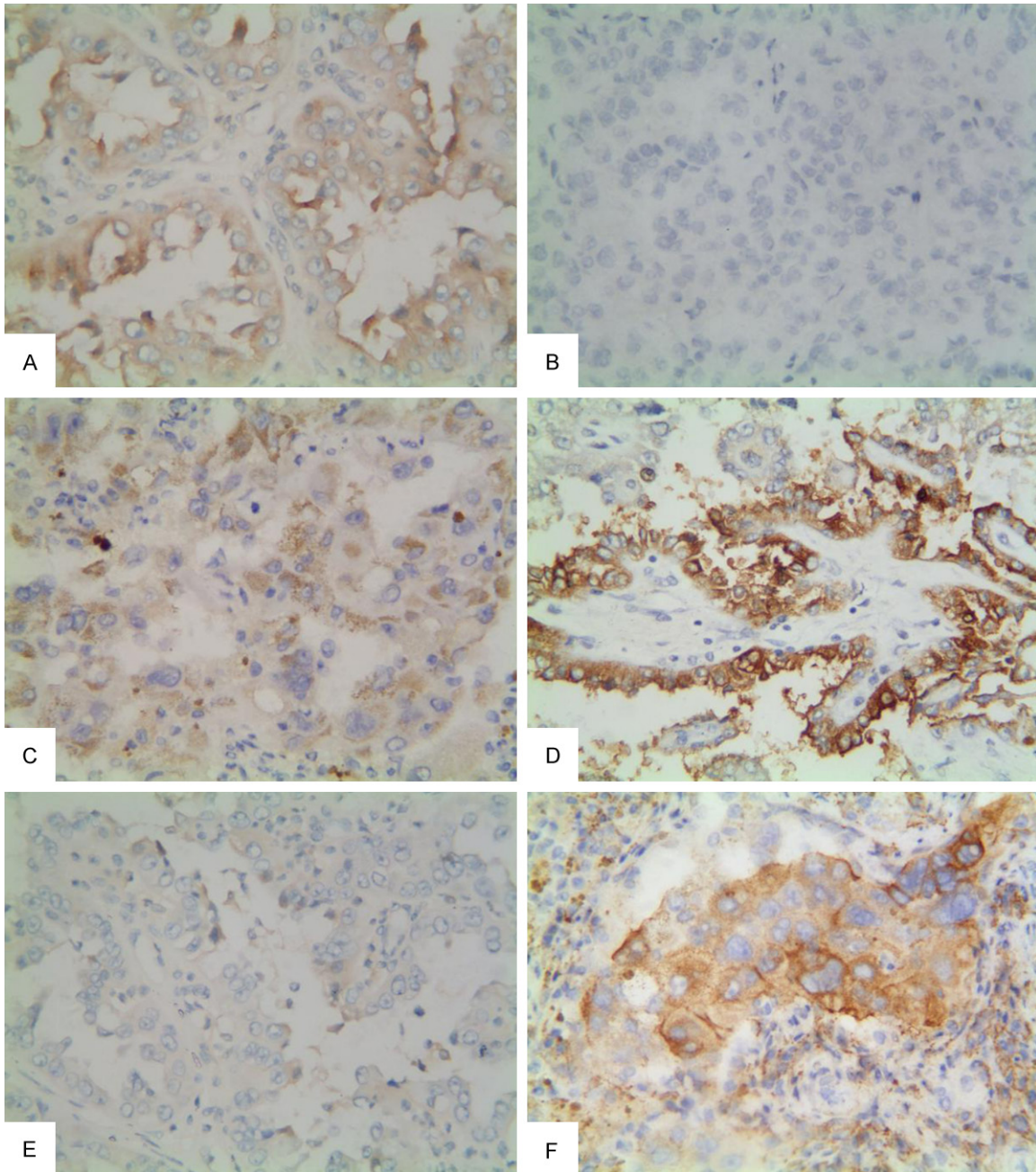


**Figure 4.** The immunohistochemical features of RCC and EMA in Xp11.2 translocation renal cell carcinoma (RCC). A. Extensive positive cytoplasmic staining for renal cell carcinoma (RCC) (light brown) in TFE3-N case (patient 2). B. Negative expression of renal cell carcinoma (RCC) in the cytoplasm in TFE3-N case (patient 4). C. Renal cell carcinoma (RCC) is weakly expressed in the cytoplasm with fine graininess in TFE3-M case (patient 5). D. Epithelial membrane antigen (EMA) is positively expressed in parts of the cell membrane and cytoplasm (dark brown), as shown in TFE3-N case (patient 1). E. Negative expression of epithelial membrane antigen (EMA) in the cytoplasm of TFE3-N case (patient 2). F. Focal expression of epithelial membrane antigen (EMA) in the cell membrane and cytoplasm. The cell membrane was stained heavily, and the cytoplasm lightly in TFE3-M case (patient 5). All magnification:  $\times 400$ .

with TFE3-N tested negative for CK7 (**Figure 5B**). However, CD10 staining was only observed in samples from TFE3-N patients (**Figure 5C, 5D; Table 3**). In patient 5, the heteromorphic

cells were of distinct sizes and of differing overall and nucleolar morphologies (**Figure 2F**). Additionally, HMB-45 expression was only detected in samples from the patient with TFE3-M

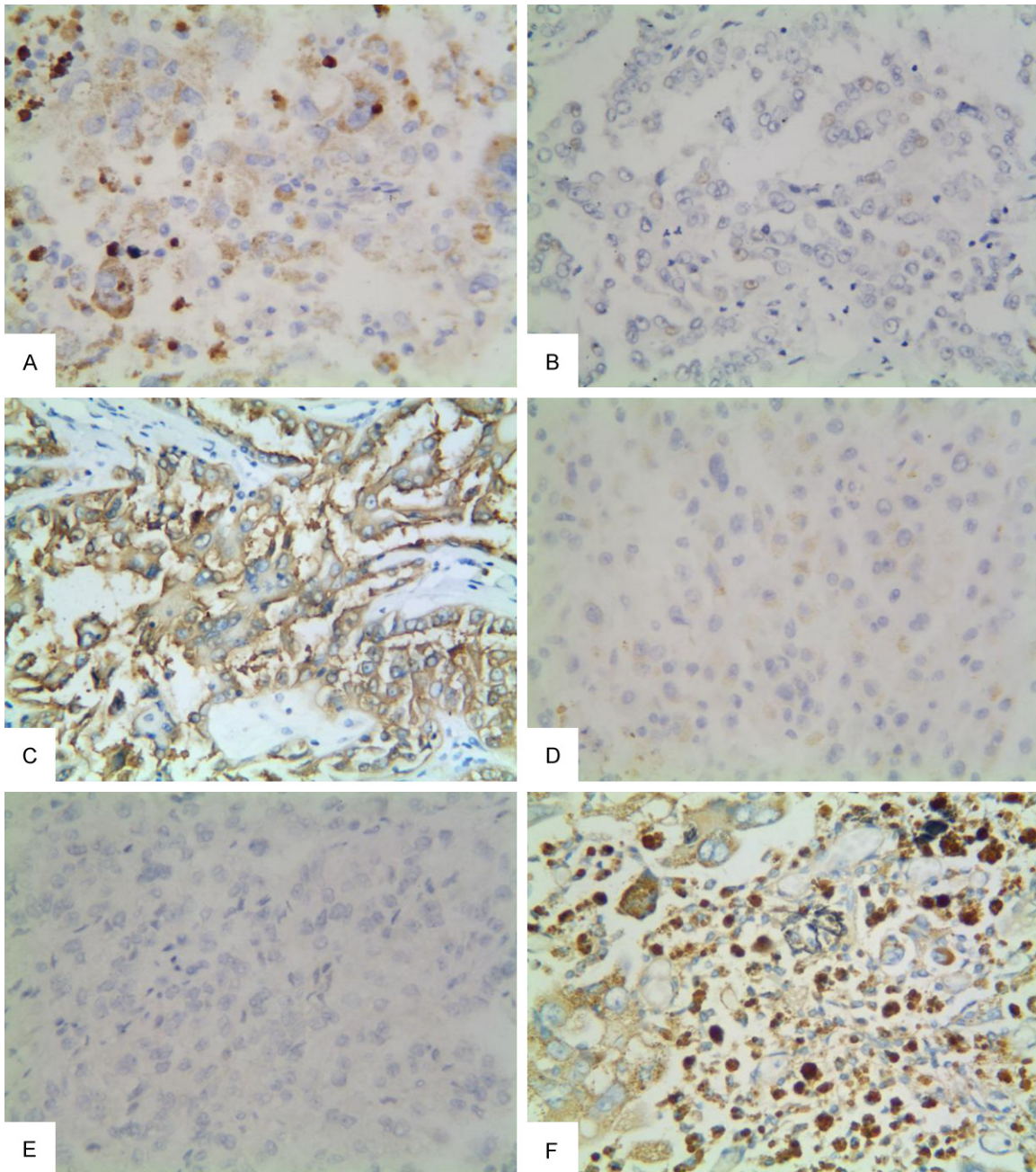


**Figure 5.** The immunohistochemical features of CK7, CD10 and HMB-45 in Xp11.2 translocation renal cell carcinoma (RCC). A. Cytokeratin 7 (CK7) is weakly expressed in the cytoplasm with fine graininess in TFE3-M case (patient 5). B. Negative expression of cytotkeratin 7 (CK7) in the cytoplasm in TFE3-N case (patient 1). C. Cluster of differentiation 10 (CD10) showed a homogeneous and diffuse positive expression in the cytoplasm (brown staining), and was lighter than P504S in TFE3-N case (patient 1). D. Negative expression of cluster of differentiation 10 (CD10) in the cytoplasm in TFE3-M case (patient 5). E. Negative expression of human melanoma black-45 (HMB-45) in the cytoplasm in TFE3-N case (patient 3). F. Human melanoma black-45 (HMB-45) is expressed in the cytoplasm (light brown) with fine graininess in TFE3-M case (patient 5). All magnification:  $\times 400$ .

(Figure 5E, 5F; Table 4), in which the tumor cells strongly expressed TFE3 and vimentin (Figure 3B and 3E).

While the number of case reports related to Xp11.2 translocation RCC is limited, we searched

PubMed and identified relevant major English-language case series that described immunohistochemistry. Argani et al. [8] reported five patients with Xp11 translocation RCC, with EMA, vimentin, CK7, and HMB-45 positivity rates of 20%, 0%, 40%, and 40% respective-

## Xp11.2 translocation/TFE3 RCC with MPP

**Table 3.** Immunohistochemistry results

Case	Type	TFE3	P504s	EMA	CD10	Vimentin	CK7	RCC	HMB-45
1	TFE-N	2+	2+	+	2+	-	-	-	-
2	TFE-N	3+	+	-	3+	3+	-	3+	-
3	TFE-N	2+	+	-	+	-	-	+	-
4	TFE-N	2+	2+	+	2+	2+	-	-	-
5	TFE-M	2+	+	+	-	2+	+/-	+	+

TFE-N, Xp11.2 translocation renal cell carcinoma (RCC) with a normal pattern; TFE-M, Xp11.2 translocation RCC with a micro-papillary pattern. TFE3, transcription factor E3; EMA, epithelial membrane antigen; CD10, cluster of differentiation 10; CK7, cytokeratin 7; HMB-45, human melanoma black-45.

**Table 4.** Comparison of immunohistochemistry results between the present study patients and those previously reported with Xp11.2 translocation RCC

Primary antibody	Present study (n = 5)	Argani et al. [7] (n = 5)	Pivovarcikova et al. [8] (n = 3)	Camparo et al. [9] (n = 29)	Bruder et al. [10] (n = 7)
TFE3	5/5 (100%)	-	2/3 (66.7%)	27/29 (93.1%)	5/7 (71.4%)
P504s	5/5 (100%)	-	-	28/29 (96.6%)	-
EMA	3/5 (60%)	1/5 (20%)	-	8/29 (27.6%)	-
CD10	4/5 (80%)	-	3/3 (100%)	26/29 (89.7%)	5/7 (71.4%)
Vimentin	3/5 (60%)	0/5 (0%)	1/3 (33.3%)	17/29 (58.6%)	-
CK7	1/5 (20%)	2/5 (40%)	1/3 (33.3%)	4/29 (13.8%)	-
RCC	3/5 (60%)	-	-	-	6/7 (85.7%)
HMB-45	1/5 (20%)	2/5 (40%)	2/3 (33.3%)	11/29 (37.9%)	-

TFE3, transcription factor E3; EMA, epithelial membrane antigen; CD10, cluster of differentiation 10; CK7, cytokeratin 7; RCC, renal cell carcinoma; HMB-45, human melanoma black-45. Not all markers were measured in all studies (as indicated by -).

ly. Pivovarcikova et al. [9] reported three patients with TFE3 RCC with TFE3, CD10, vimentin, CK7, and HMB-45 positivity rates of 66.7%, 100%, 33.3%, 33.3%, and 33.3%, respectively. Camparo et al. [10] reported 29 patients with TFE3 RCC with TFE3, P504s, EMA, CD10, vimentin, CK7, and HMB-45 positivity rates of 93.1%, 96.6%, 27.6%, 89.7%, 58.6%, 13.8%, and 37.9%, respectively. Bruder et al. [11] reported three patients with TFE3 RCC with TFE3, CD10, and RCC positivity rates of 71.4%, 71.4%, and 85.7%, respectively. **Table 4** compares our patients to those described in previous publications. Notably, the few patients with Xp11.2 translocation RCCs described to date all had tumors expressing CK7 and HMB-45.

### Karyotypes

The four specific solid single bands of TFE3-N patients have been detected which were the products of *ASPSCR1-TFE3* fusion gene. While the one specific solid single band of TFE3-M patient has been detected which was the product of *PRCC-TFE3* fusion gene (**Figure 6**),

thus revealing these patients' corresponding karyotypes.

### Discussion

#### *Epidemiological and clinical characteristics of Xp11.2 translocation RCC*

The incidence of TFE3 RCC is higher in children than in adults; its prognosis is also better in children [11, 12]. Clinically, patients with Xp11.2 translocation RCC are typically admitted to the hospital because of hematuria, abdominal pain, or an abdominal mass, and the presence of occupying lesions is confirmed using radiography, kidney color doppler ultrasonography, and CT. As this presentation is similar to that of common adult RCC subtypes such as conventional clear cell RCC and papillary RCC (*PRCC*), the frequency of Xp11.2 translocation RCCs in adults may be underestimated. One single-institution study subjected 433 adult patients to cytogenetics and TFE3 immunohistochemical analyses and found that Xp11.2 translocation RCCs accounted for 1.6% of the cases [13]. In our study, all five patients

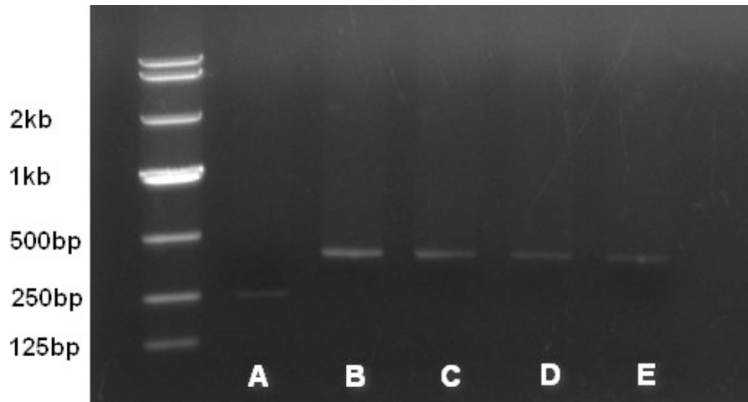


**Figure 6.** Detection of Xp11.2 translocation renal cell carcinoma (RCC) by RT-PCR. A. Detection of PRCC-TFE3 fusion gene product by RT-PCR of paraffin tissue from the single TFE3-M patient. B-E. Detection of ASPSCR1-TFE3 fusion gene products by RT-PCR of paraffin tissue from the four TFE3-N patients.

were adults with initial symptoms such as back pain, painless hematuria, and the presence of an occupying mass in the kidney; these symptoms are consistent with previous reports in the literature.

Exposure to chemotherapy is a known risk factor for Xp11.2 translocation RCC, and up to 15% of patients with this disease have a history of such exposure [14]. Although chemotherapeutic agents have varying mechanisms of action, most cytotoxic agents cause DNA damage that might consequently initiate a repair process that in turn could facilitate a chromosomal translocation. However, none of the five patients in our study had previously been exposed to chemotherapy or reported other comorbidities; therefore, the etiologies of their diseases remain unknown.

#### *Histopathology and immunohistochemistry*

The gross features of Xp11.2 translocation RCC are similar to those of conventional clear cell RCC. Macroscopically, the cut surfaces of the tumors are greyish-yellow in color and exhibit hemorrhaging and necrosis. Morphologically, the tumors comprise a combination of nested and papillary structures with clear-to-granular eosinophilic cytoplasm. In contrast, the different subtypes of Xp11.2 translocation RCC are histopathologically distinct. Typically, cells of the alveolar soft part sarcoma chromosome region (*ASPSCR1*)-*TFE3* subtype are characterized by a higher amount of clear-to-eosinophilic cytoplasm relative to the other subtypes, and

exhibit discontinuous cell boundaries, vesicular nuclei, and obvious nucleoli. In contrast, the typical features of *PRCC-TFE3* Xp11.2 translocation RCC include a diminished cytoplasm, fewer psammoma bodies and hyaline globules, and a more nested structure [1].

In patient 5 (with TFE3-M), histopathological features such as less abundant cytoplasm and a more compact nested growth pattern of the MPP component suggest a *PRCC* subtype. In contrast, tumors from the four TFE3-N patients exhibited abundant cytoplasm

and a papillary structure indicative of the *ASPSCR1* subtype. Despite these characteristics, RT-PCR was used to determine the karyotype by detecting the expression of fusion gene, thus this assay is utility in the diagnosis of relevant diseases [15].

RT-PCR was performed to confirm the presence of an *ASPSCR1-TFE3* and *PRCC-TFE3* fusion transcript by using forward primers from the *ASPSCR1* and *PRCC* sequence and a reverse primer from *TFE3* exon. The image result (**Figure 6**) showed specific *ASPSCR1-TFE3* and *PRCC-TFE3* products which confirmed the diagnosis of TFE3 RCC and also identified the relevant karyotypes [16, 17]. The karyotypes of four TFE3-N patients and one TFE3-M patient are *ASPSCR1-TFE3* and *PRCC-TFE3*, respectively.

Xp11.2 translocation RCC cells downregulate the expression of epithelial markers such as CKs and EMA, but constitutively express RCC markers such as RCC and PAX8 [13]. Unusual subtypes of Xp11.2 translocation RCC, such as *PSF-TFE3* and *CLTL-TFE3* RCCs, can express melanocytic markers such as melan-A and HMB-45 [18]. In approximately half of all affected patients, Xp11.2 translocation RCC cells express the cysteine protease cathepsin K, which is also expressed in perivascular epithelioid carcinomas [19]. In our study, all five patients with Xp11.2 translocation RCC were positive for both TFE3 and P504S, as consistent with the literature. Notably, HMB-45 and weak CK7 expression were only detected in

patient 5 (TFE3-M), who was the only patient negative for CD10. These findings, as well as those from other studies (**Table 4**), might be related to differences between the *ASPSCR1* and *PRCC* subtypes. Given the rarity of Xp11.2 translocation RCC, further investigations ought to determine whether immunohistochemical differences are characteristic of RCC subtypes.

Regarding the cytology of Xp11.2 translocation RCC, we found that more heteromorphic nuclei increased the likelihood that the nucleolus would be located in the center of the neoplasm cell. In other words, the visibility of the nucleolus appears to correlate with the proliferative ability of the cell. This tendency is consistent with tumor cell behavior, as malignant tumors have higher proliferative ability than benign tumors.

### Genetics

The 2013 International Society of Urologic Pathology Vancouver classification of renal neoplasia classified Xp11.2 translocation RCCs and t(6;11) RCCs as MiT family translocation RCCs [20]. The MiT subfamily of transcription factors includes MiTF, TFE3, TFEB, and TFEC, which share homologous DNA-binding and -activation domains. Mechanistically, t(6;11) RCCs are caused by *TFEB* translocation, whereas *MiTF* translocation can also occur in MiTF RCCs. Therefore, the related literature refers to these conditions as MiTF/TFE family RCCs.

The pairing of MiT family transcription factors with their gene fusion partners can yield fusion proteins. The reported fusion partners of *TFE3* transcription factors include *ASPSCR1*, *PRCC*, *PSF*, *NONO* and *CLTC*, which are located on chromosomes 17q25, 1q21, 1p34, Xq12, and 17q23, respectively. Of these, the most common partners, *ASPSCR1* and *PRCC*, correspond to Xp11.2 translocation RCC subtypes. Although *Alpha*, an intronless gene, has been reported as a fusion partner of *TFEB*, no fusion partners have been reported for *MiTF*. In the present study, the TFE3-M patient was thought to be of the *PRCC* subtype given the characteristic structure of the MPP. In contrast, the TFE3-N patients were likely to be of the *ASPSCR1* subtype, given the conventional RCC structure. We deduce that the *PRCC* fusion partner correlates with the MPP structure.

Other specific features of the TFE3-M patient in our study included the significant deposition of melanin particles and expression of HMB-45. These features are characteristic of melanoma but have never previously been reported in an Xp11.2 translocation RCC. Accordingly, these features may be related to MiTF, which typically promotes the expression of melanocytic lineage differentiation markers such as cathepsin K and HMB-45 [21]. As noted above, both MiTF and TFE3 belong to the MiT family and share a certain homology regarding the expression of melanoma-related proteins. Thus, we speculate that the histological characteristics of all Xp11.2 translocation RCCs (i.e., not only TFE3-M) are multifactorial and depend on various MiT family transcription factors and their gene fusion partners. Further studies of Xp11.2 translocation RCCs with novel histological features that could be linked to other MiT family transcription factors or their gene fusion partners are required to confirm this hypothesis.

### Conclusion

Xp11.2 translocation RCCs are rare and, to the best of our knowledge, a tumor of this type with an MPP has not been previously reported. Unlike other neoplasms with MPPs, the TFE3-M patient in our study exhibited a good prognosis and also had unique morphologic features, including small papillae, melanin particle deposition interspersed in the acinar and lacunar spaces, and positive HMB-45 expression. The etiology of all Xp11.2 translocation RCCs (irrespective of the presence of an MPP) is likely multifactorial and related to the MiT family transcription factors and their gene fusion partners. Therefore, the characteristic histologic features of Xp11.2 translocation RCCs should be considered distinct from those of conventional RCCs, not similar to them as previously reported. Xp11.2 translocation RCC should be considered when tumors exhibit a suspicious pattern. Our findings may also help establish a specific category of diseases encompassing Xp11.2 translocation and other rare RCCs that share histologic features associated with MiT family transcription factors and their gene fusion partners. Such an integrated category may facilitate the clinical diagnosis and treatment of such rare RCCs going forward.

### Acknowledgements

This work was supported by the Nature Science Foundation of Anhui Province (No. 140808-

5MH147), the Nature Science Key Program of Colleges and Universities of Anhui Province (No. KJ2016A460), and the Key Projects of Support Program for Outstanding Young Talents in Colleges and Universities of Anhui Province (No. gxyq2017032).

#### Disclosure of conflict of interest

None.

**Address correspondence to:** Yi-Sheng Tao and Da-Min Chai, Department of Pathology, The First Affiliated Hospital of Bengbu Medical College, Bengbu, Anhui, China. E-mail: taoyishengbbyxy@163.com (YST); msautumn@163.com (DMC); Z Peter Wang, Department of Pathology, Beth Israel Deaconess Medical Center, Harvard Medical School, Boston, MA, USA. E-mail: zwang6@bidmc.harvard.edu

#### References

- [1] Argani P, Antonescu CR, Couturier J, Fournet JC, Sciot R, Debiec-Rychter M, Hutchinson B, Reuter VE, Boccon-Gibod L, Timmons C, Hafez N, Ladanyi M. PRCC-TFE3 renal carcinomas: morphologic, immunohistochemical, ultrastructural, and molecular analysis of an entity associated with the t(X;1)(p11.2;q21). *Am J Surg Pathol* 2002; 26: 1553-1566.
- [2] Argani P, Antonescu CR, Illei PB, Lui MY, Timmons CF, Newbury R, Reuter VE, Garvin AJ, Perez-Atayde AR, Fletcher JA, Beckwith JB, Bridge JA, Ladanyi M. Primary renal neoplasms with the ASPL-TFE3 gene fusion of alveolar soft part sarcoma: a distinctive tumor entity previously included among renal cell carcinomas of children and adolescents. *Am J Pathol* 2001; 159: 179-192.
- [3] Silver SA, Askin FB. True papillary carcinoma of the lung: a distinct clinicopathologic entity. *Am J Surg Pathol* 1997; 21: 43-51.
- [4] Cha MJ, Lee HY, Lee KS, Jeong JY, Han J, Shim YM, Hwang HS. Micropapillary and solid subtypes of invasive lung adenocarcinoma: clinical predictors of histopathology and outcome. *J Thorac Cardiovasc Surg* 2014; 147: 921-928, e2.
- [5] Amin MB, Tamboli TP, Merchant SH, Ordóñez NG, Ro J, Ayala AG, Ro JY. Micropapillary component in lung adenocarcinoma: a distinctive histologic feature with possible prognostic significance. *Am J Surg Pathol* 2002; 26: 358-364.
- [6] Wu S, Yu L, Wang D, Zhou L, Cheng Z, Chai D, Ma L, Tao Y. Aberrant expression of CD133 in non-small cell lung cancer and its relationship to vasculogenic mimicry. *BMC Cancer* 2012; 12: 535.
- [7] Macher-Goeppinger S, Roth W, Wagener N, Hohenfellner M, Penzel R, Haferkamp A, Schirmacher P, Aulmann S. Molecular heterogeneity of TFE3 activation in renal cell carcinomas. *Mod Pathol* 2012; 25: 308-315.
- [8] Argani P, Zhong M, Reuter VE, Fallon JT, Epstein JI, Netto GJ, Antonescu CR. TFE3-fusion variant analysis defines specific clinicopathologic associations among Xp11 translocation cancers. *Am J Surg Pathol* 2016; 40: 723-737.
- [9] Pivovarcikova K, Grossmann P, Alaghebandan R, Sperga M, Michal M, Hes O. TFE3-fusion variant analysis defines specific clinicopathologic associations among Xp11 translocation cancers. *Am J Surg Pathol* 2017; 41: 138-140.
- [10] Camparo P, Vasiliu V, Molinie V, Couturier J, Dykema KJ, Petillo D, Furge KA, Comperat EM, Lae M, Bouvier R, Boccon-Gibod L, Denoux Y, Ferlicot S, Forest E, Fromont G, Hintzy MC, Laghouati M, Sibony M, Tucker ML, Weber N, Teh BT, Vieillefond A. Renal translocation carcinomas: clinicopathologic, immunohistochemical, and gene expression profiling analysis of 31 cases with a review of the literature. *Am J Surg Pathol* 2008; 32: 656-670.
- [11] Bruder E, Passera O, Harms D, Leuschner I, Ladanyi M, Argani P, Eble JN, Struckmann K, Schraml P, Moch H. Morphologic and molecular characterization of renal cell carcinoma in children and young adults. *Am J Surg Pathol* 2004; 28: 1117-1132.
- [12] Geller JI, Ehrlich PF, Cost NG, Khanna G, Mullen EA, Gratias EJ, Naranjo A, Dome JS, Perlman EJ. Characterization of adolescent and pediatric renal cell carcinoma: A report from the Children's Oncology Group study AREN03B2. *Cancer* 2015; 121: 2457-2464.
- [13] Komai Y, Fujiwara M, Fujii Y, Mukai H, Yonese J, Kawakami S, Yamamoto S, Migita T, Ishikawa Y, Kurata M, Nakamura T, Fukui I. Adult Xp11 translocation renal cell carcinoma diagnosed by cytogenetics and immunohistochemistry. *Clin Cancer Res* 2009; 15: 1170-1176.
- [14] Argani P, Laé M, Ballard ET, Amin M, Manivel C, Hutchinson B, Reuter VE, Ladanyi M. Translocation carcinomas of the kidney after chemotherapy in childhood. *J Clin Oncol* 2006; 24: 1529-1534.
- [15] Ladanyi M, Lui MY, Antonescu CR, Krause-Boehm A, Meindl A, Argani P, Healey JH, Ueda T, Yoshikawa H, Meloni-Ehrig A. The der(17)t(X;17)(p11;q25) of human alveolar soft part sarcoma fuses the TFE3 transcription factor gene to ASPL, a novel gene at 17q25. *Oncogene* 2001; 20: 48-57.
- [16] Aulmann S, Longerich T, Schirmacher P, Mechttersheimer G, Penzel R. Detection of the ASPSCR1-TFE3 gene fusion in paraffin-embedded alveolar soft part sarcomas. *Histopathology* 2007; 50: 881-886.

## Xp11.2 translocation/TFE3 RCC with MPP

- [17] Lee HJ, Shin DH, Noh GY, Kim YK, Kim A, Shin N, Lee JH, Choi KU, Kim JY, Lee CH, Sol MY, Rha SH, Park SW. Combination of immunohistochemistry, FISH and RT-PCR shows high incidence of Xp11 translocation RCC: comparison of three different diagnostic methods. *Oncotarget* 2017; 8: 30756-30765.
- [18] Argani P, Lui MY, Couturier J, Bouvier R, Fournet JC, Ladanyi M. A novel CLTC-TFE3 gene fusion in pediatric renal adenocarcinoma with t(X;17)(p11.2;q23). *Oncogene* 2003; 22: 5374-5378.
- [19] Martignoni G, Gobbo S, Camparo P, Brunelli M, Munari E, Segala D, Pea M, Bonetti F, Illei PB, Netto GJ, Ladanyi M, Chilosì M, Argani P. Differential expression of cathepsin K in neoplasms harboring TFE3 gene fusions. *Mod Pathol* 2011; 24: 1313-1319.
- [20] Srigley JR, Delahunt B, Eble JN, Egevad L, Epstein JI, Grignon D, Hes O, Moch H, Montironi R, Tickoo SK, Zhou M, Argani P; ISUP Renal tumor panel. The international society of urological pathology (ISUP) vancouver classification of renal neoplasia. *Am J Surg Pathol* 2013; 37: 1469-1489.
- [21] Argani P. MiT family translocation renal cell carcinoma. *Semin Diagn Pathol* 2015; 32: 103-113.